FUDMA Journal of Renewable and Atomic Energy (FJoRAE)
ISSN: 3027-2335
Vol. 1 No 2, June 2024. Pp 79-91

https://doi.org/10.33003/fjorae.2024.0102.06

Optimization of TiO_2 Nanostructure Antireflection Coatings for Enhanced Optical Performance in $GaAs$ Solar Cells

[1]S. D. Muhammad and M. H. Ali
National Environmental Standards Regulations and Enforcement Agency, Department of Physics, Bayero University, Kano

Abstract

This study presents the effects of the various titanium dioxide (TiO_2) nanostructures as anti-reflection coatings on solar cells. The study is conducted in the COMSOL Multi-physics environment where $GaAs$ solar cell and titanium dioxide based antireflection coating are simulated. The optical properties of the solar cells with and without the coating were evaluated. Three different coating particles were used; cubic, spherical and pyramidal. The simulation results showed that the cubic nanostructure was found to be more effective, reducing the reflectance percentage from 25.5% without ARC to 3.55% with the ARC at a dimension of 50 nm. The pyramidal nanostructure at same width and a height of 100 nm also demonstrated a reduction in reflectance to 9.9%. This result will definitely enhance the absorption capability of the solar cell whereby increasing its overall efficiency.

Keywords: Antireflection, Coating, COMSOL, Nanostructure, Solar cell, Titanium dioxide

1. Introduction

The front surface of photovoltaic (PV) modules is crucial, accounting for a significant portion of the total module cost (Shanmugam et al., 2020). It serves as a protective barrier for the delicate PV cells against external damage such as abrasion, water, dirt, and soiling. According to the Fresnel reflection formula, approximately 4% of sunlight is reflected by the front of the panel glass, which does not contribute to photon generation (Law et al., 2023). To mitigate this reflection loss, single-layer or multiple-layer anti-reflection coatings ($ARCs$) are commonly used.

Various materials have been utilized in designing these $ARCs$ for photovoltaic solar cells, such as Silica (SiO_2), Magnesium Fluoride (MgF_2), Zinc Oxide (ZnO) e.t.c. Silica being the most widely used due to its abundance, low cost, stability, and non-toxicity (Rathanasamy *et al.* 2022) but it required multiple layers to achieve desirable antireflection performance. Likewise, according to Makableh et al. (2021) MgF_2 and ZnO has the drawback of less durability and prone to degradation under UV exposure respectively. However, the high refractive index of about 2.4-2.7 depending on the crystalline phase (Anatase or Rutile) and energy band gap of 3.2eV-3.4eV of titanium dioxide (TiO_2)

[1] Corresponding Author's e-mail: sunusidayyab@gmail.com, mhali.phy@buk.edu.ng

made it more acceptable than other ARC materials. However, its photocatalytic and durability allow TiO_2 nanoparticles to offer self-cleaning properties due to their highly hydrophobic nature, facilitating the removal of dirt through droplet sliding, or their hydrophilic nature, which forms a water film that prevents adhesion (Richards, 2003). These nanoparticles also exhibit excellent electrical, optical, and anti-fogging properties, making them a favorable choice for anti-reflection coatings that reduce reflection loss.

To further reduce reflection loss, many researchers have adopted multi-layer ARC coatings. However, these coatings, composed of thin-film dielectric layers, which present challenges such as material mismatch issues where choosing a materials with appropriate refractive indices and compatibility remain a difficult task, and sensitivity to thickness variations in which any deviation can significantly reduce the effectiveness of the layers, as such the coating may develop undesired optical properties such as scattering and absorption (Mandong & Uzum, 2021). Furthermore, Womack et al., (2017) highlighted that the fabrication of multilayers coating often required sophisticated deposition techniques such as Chemical Vapor Deposition (CVD) which can be complex and costly. As an alternative, different material in nanostructures have been used to design single-layer $ARCs$ to overcome these challenges. However, the optical properties of these nanostructures are yet to be fully evaluated.

Researchers continue to enhance the efficiency of photovoltaic solar cells by minimizing reflection loss and maximizing the absorption at the front surface of the solar cells. Rathanasamy et al., (2022) focused on improving the power conversion efficiency of polycrystalline silicon solar cells using single and double-layer $ARCs$ deposited via the electro-spraying technique. It found that while double-layer $ARCs$ are expensive, they reduce reflectance to 9.6%. Another study optimized the dimensions of three TiO_2 nanostructures (cubic, pyramidal, and spherical) coated on solar cells, revealing that spherical shapes could reduce reflectance from 37.2% without ARC to 9.2% at the radius of 25 nm (Abu-Shamleh et al., 2021). Domtau et al., (2016) examined the effect of TiO_2 film thickness on the optical and electrical properties of thin films coated on glass substrates, noting that reflectance, absorption, band gap, and refractive index increase with film thickness, while transmission decreases. Furthermore, the work of Leem et al. (2014) demonstrated that the optical reflection properties of single-junction solar cells in the wavelength range of 350-900 nm at incident light angles of 3^0-80^0 which showed that a 50 nm TiO_2 nanostructure could reduce reflection to 6.2% compared to cells without ARC.

In this work, the effects of three TiO_2 nanostructures (spherical, cubic, and pyramidal) on the solar cell's optical properties were evaluated using COMSOL Multi-physics software. The results would aid in designing a reliable single-layer ARC for solar cells efficiency improvement.

2. Theoretical Background

Optical reflection is a fundamental phenomenon that occurs when light passes across a boundary between two media with different refractive indices. In the design of photovoltaic solar cells, the anti-reflection coating (ARC) and the solar cell (substrate) are two such media through which light propagates which later converted into electricity. ARC reduces reflection and enhances the absorption of light, thereby boosting the photoelectric conversion process. Consequently, various $ARCs$ are designed to improve the efficiency of solar cells. Among these, quarter-wavelength $ARCs$ are particularly effective, relying on the wavelength, refractive index of the coating material, coating thickness, and angle of incidence. If the refractive index of the ARC is n_{ARC} and the free space wavelength is λ , the optimum thickness of the coating layer can be calculated as (Mbengue et al., 2016).

$$d = {}^{\lambda}/_{4n_{ARC}} \tag{1}$$

The refractive index of the ARC (TiO_2) can also be obtain as (Wang & Shen, 2010)

$$n_{ARC} = \sqrt{n_0 \times n_s} \tag{2}$$

where n_0 his refractive index of air (1.0) and n_s is the refractive index of the substrate that is $GaAs$ solar cell.

However, nanostructures ARC significantly influence the optical properties such as reflection, refraction and absorption where it modify these processes.

Furthermore, the nanostructures create a graded refractive index profile from air to the TiO_2 layer. This gradual transition reduces the abrupt change in refractive index at the surface, leading to reduced reflection. In addition to that, if the wavelength of the nanostructures are smaller than that of incident light, they act as an effective medium with a refractive index between air and TiO_2, thereby reducing reflectance due to destructive interference.

The schematic diagram of the layers taking place in the reflection process of the light energy through the ARC layer is shown in Figure. 1.

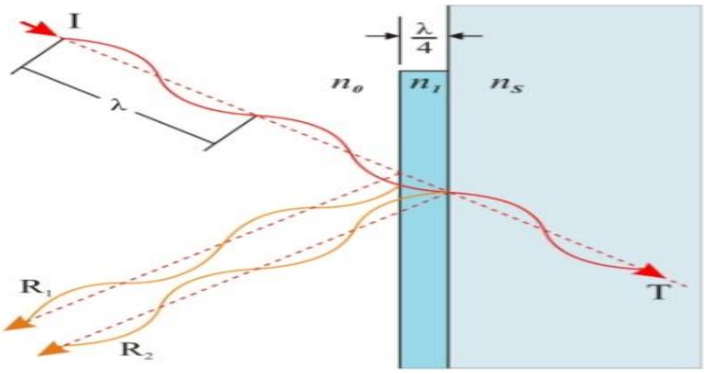

Figure 1: Interference of light through the ARC layer(Parajuli et al., 2023)

The reflection coefficients on the first and second surfaces are given in terms of the refractive indices as;

$$r_1 = \frac{n_0+n_{ARC}}{n_0+n_{ARC}}, \quad r_2 = \frac{n_{ARC}-n_S}{n_{ARC}+n_S} \tag{3}$$

The resultant reflectivity (equivalent to a single layer) is given by:

$$R = |r_2| = \frac{r_1^2+r_2^2+2r_1r_2\cos 2\theta}{1+r_1^2r_2^2+2r_1r_2\cos 2\theta} \tag{4}$$

The optical path difference is obtained by using equation (5)

$$\theta = \frac{2\pi d n_{ARC}}{\lambda} \tag{5}$$

The interface between the coating and the substrate can be homogeneous or heterogeneous depending on their refractive indices and energy band. Therefore, the $TiO_2/GaAs$ interface is heterogeneous by virtue of their properties. However, as reported by Parajuli et al. (2023), the high refractive index (3.3-3.6) and indirect energy band gap with high electron mobility ($9000cm^2/V$) of $GaAs$ solar cell substrate indicated the superiority than other materials such as silicon and perovskite because it possess higher absorption coefficient and a larger charge transfer capacity even when expose to high temperature.

3. Structural Design and Simulation Details

The three most common TiO_2 nanostructures (cubic, spherical, and pyramidal) can be fabricated or grown on solar cell substrates using the modern deposition techniques such as sol-gel method. In this work, a single-layer TiO_2 nanostructure is designed (simulated) to sit on a solar cell substrate, surrounded by air with a refractive index of one. The effective refractive index varied due to effective area of the three nanostructures changes vertically and the roughness of the substrate surface.

Therefore, to achieve a diverse optical properties, the complex refractive indices of TiO_2 and the solar cell are defined based on effective medium theory which can be calculated using equation (6).

$$n_{eff} = \sqrt{n^2_{bulk(ARC)} \times FF + n^2_{air}(1 - FF)} \quad (6)$$

Where n_{eff} is the effective refractive index, $n_{bulk(ARC)}$ is the refractive index of TiO2 (2.7), n_{air} is the refractive index of air and FF is the filling factor. The filling factor is defined as the ratio of the area of the nanostructure shape to the area of the surrounding rectangular shape. The filling factor is less than one for spherical and pyramidal shapes, while it is zero for cubic structures. Figure 2 illustrates how to calculate the filling factor for these shapes.

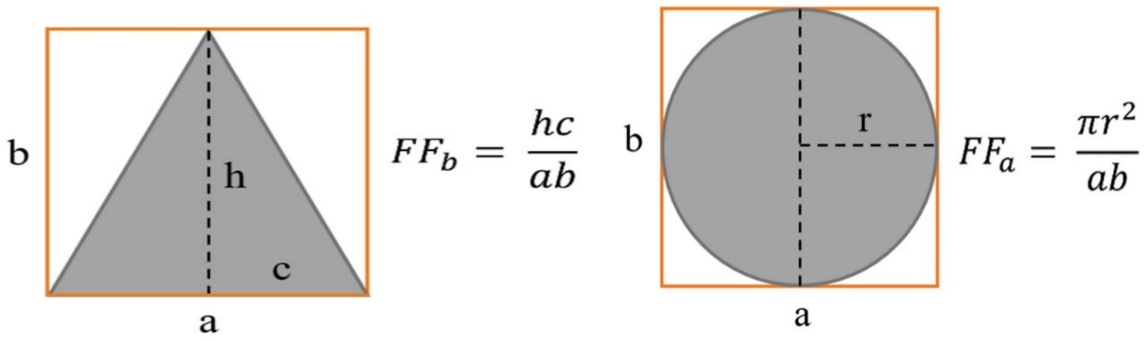

Figure 2: Pyramidal and spherical shape of nanostructure(Abu-Shamleh et al., 2021)

During the simulation, the two-dimensions were selected based on previous literature (Abu-Shamleh et al., 2021)(Parajuli et al., 2023)(Makableh et al., 2021) and then optimized through multiple runs. The dimensions of the substrate and the surrounding air were set at 300 nm and 150 nm in length, respectively. However, the optimized dimensions of the selected shapes were determined based on width, length, and radius, as shown in Table 1.

Furthermore, before simulating the optical effects of geometrical factors on nanoparticles, the reflectance of the solar cell across different wavelengths ranging from 400 nm to 800 nm without antireflection coatings was simulated as a reference value.

Table 1: Dimension of the three selected TiO_2 nanostructure

Geometry	Dimension
Cubic of different length	l= 100nm l=80nm l=50nm
Pyramid	w=100nm w=80nm

At constant height of 80nm	w=50nm
Pyramid At constant width of 50nm	h=100nm h=80nm h=50nm
Sphere of different radius	r=50nm r=35nm r=25nm

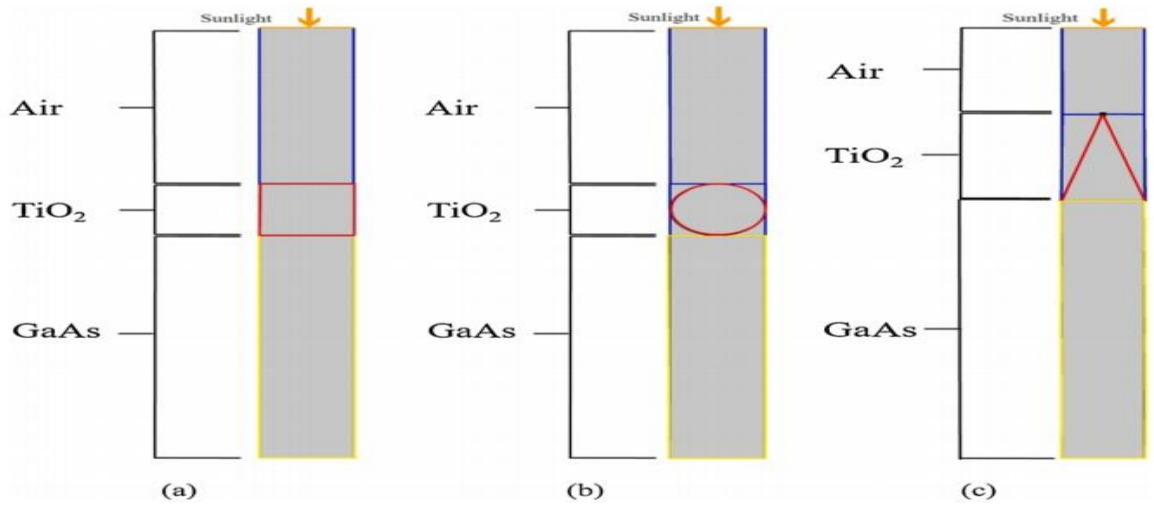

Figure 3: The diagram of $GaAs$ coated with the selected TiO_2 nanostructures(Abu-Shamleh et al., 2021)

The boundary conditions for the electromagnetic wave frequency domain were appropriately defined during the simulation. The two vertical sides of the domain were assigned periodic boundary conditions, while the ARC domain was designated as a perfectly matched layer to present artificially absorbing boundaries and prevent unwanted field reflections. Four periodic ports were assigned at the upper and bottom boundaries of the air and substrate domains to implement the electromagnetic field source, with the wave excitation slit port activated only in the air domain. Moreover, the slit condition of the interior ports at the upper and bottom of the ARC was activated before applying the free triangular finer mesh to the entire domain. The mesh densities of the three layers were set differently by refining the mesh size based on the layers geometry, so that the accuracy of the simulated result can be ascertain. Finally, to reduce the error in computation the adaption and error estimation were selected. Most of the material properties for all domains were extracted from the COMSOL Multi-physics version 5.6 library.

Table 2: Parameter values of $GaAs$ solar cell from COMSOL Multi-physics version 5.6 library

Property	Variable	Unit
Relative permittivity	13.1	
Refractive index of real part	3.9	
Band gap	1.42	eV
Young's modulus	85.9×10^{-9}	Pa
Coefficient of thermal expansion	5.7×10^{-6}	K^{-1}
Heat capacity at constant pressure	550	J/KgK
Density	5316	Kg/m^3
Thermal conductivity	33	W/mK
Poisson ratio	0.31	
Electron Affinity	4.07	$KJ/mole$
Effective density of state valence	8.87×10^{18}	cm^{-3}
Effective density of state conduction	4.45×10^{17}	cm^{-3}
Electron mobility	8800	cm^2/Vs
Hole mobility	400	cm^2/Vs

4. Result and Discussion

The wavelength range between 400 and 800 nm represents the light spectrum absorbed and converted by solar cells into useful energy. Therefore, this spectral range was selected based on its relevance to solar cell efficiency, as reported in the literature. The reflectance percentage of the solar cell without ARC was measured at six different angles of incidence, with the intervals of 5^0, as shown in Figure 3. The lowest reflectance percentage was obtained as 25.5% at 70^0 within 600nm to 650nm band.

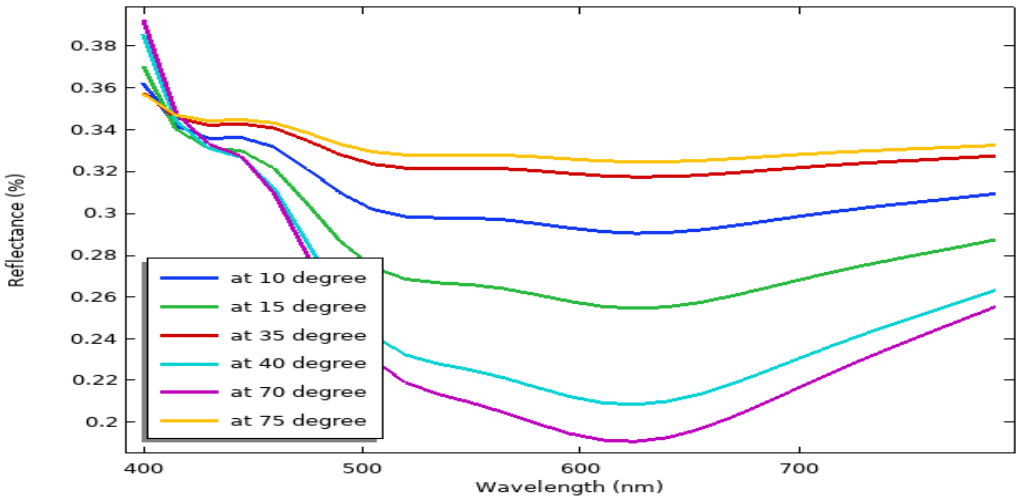

Figure 4: The reflectance percentage of $GaAs$ solar cell without ARC at different angles

After optimization of the angles of incidence of light, as well as the dimensions and thickness of the coated solar cells with the three selected nanostructures (spherical, cubic, and pyramidal). The spherical shape was found to scatter incoming light in multiple directions, increasing the likelihood of light absorption by the solar cell. It also created a graded refractive index at the surface of the solar cell, gradually reducing the refractive index from air to the substrate, thus minimizing reflection. Figure 4 shows the percentage reflectance of the spherical TiO_2 nanostructure, which was found to be 15.2%, 15.7%, and 14.3% at radii of 35 nm, 25 nm, and 50 nm, respectively.

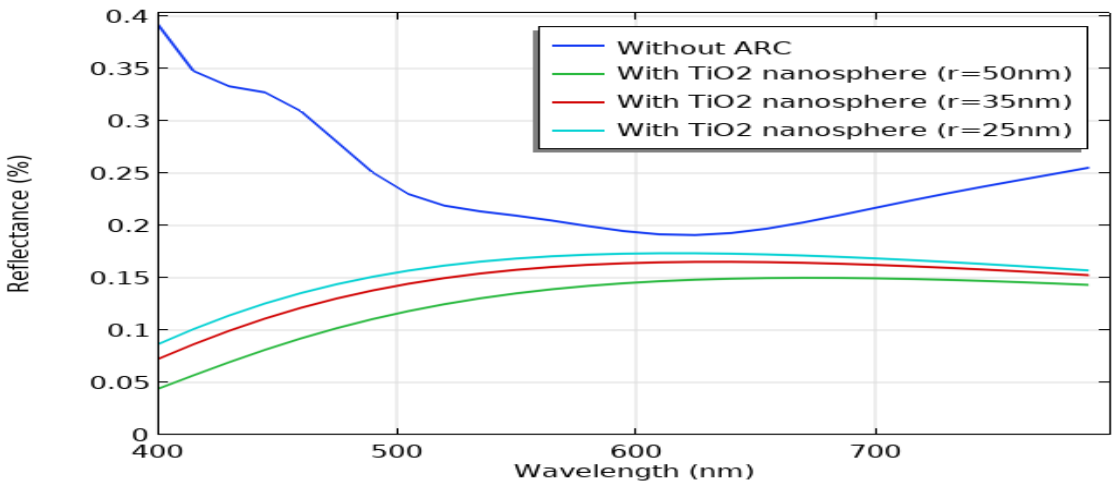

Figure 5: The reflectance percentage of $GaAs$ solar cell coated with TiO_2 nanosphere

Due to its symmetrical shape, the spherical structure can reduce reflectivity across a wide range of wavelengths and angles of incidence.

ISSN: 3027-2335

In the case of the pyramidal structure, it creates a continuous refractive index gradient and multiple internal reflections, as the pointed tips and sloped sides assist in light trapping. This gradual change in refractive index from the tip to the base helps minimize reflectivity. Additionally, the vertical tip (height) and horizontal base (width) of the pyramidal structure were optimized. The minimum reflectance percentages were found to be 14.3%, 14.9%, and 15.7% at widths of 100 nm, 80 nm, and 50 nm, respectively, with a constant height of 80 nm as shown in Figure 6.

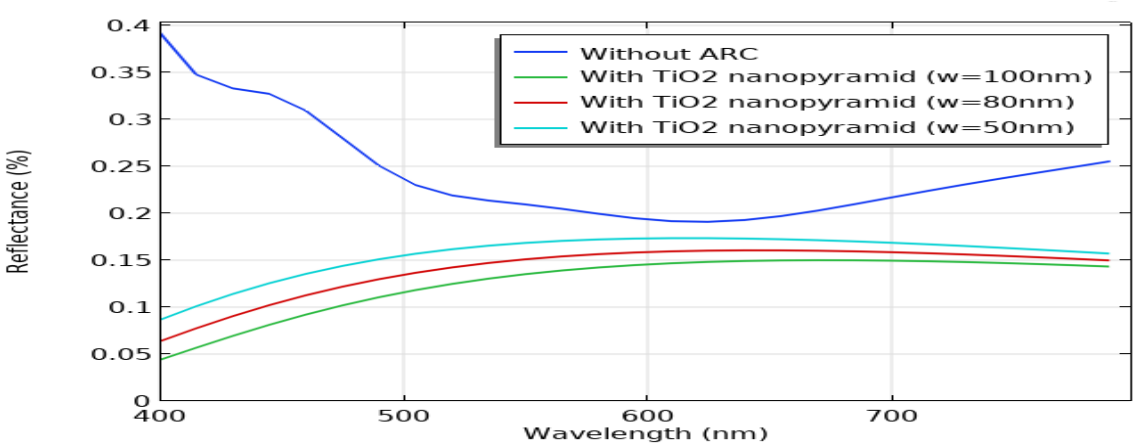

Figure 6: The reflectance percentage of $GaAs$ solar cell coated with TiO_2 nanopyramid at constant height

However, at a constant width of 50 nm, the percentage reflectance decreased to 9.9%, 12.5%, and 15.7% for heights of 100 nm, 80 nm, and 50 nm, respectively as shown in Figure 7. No reduction in reflectance was observed at the (width = 50 nm, height = 80 nm) and (width = 50 nm, height = 50 nm) configurations. A significant reduction in reflectance was noted between (width = 100 nm, height = 80 nm) and (width = 50 nm, height = 100 nm). The 9.9% reflectance represents the lowest reduction achieved by the pyramidal structure compared to the spherical structure, as illustrated in Figures 5 and 6.

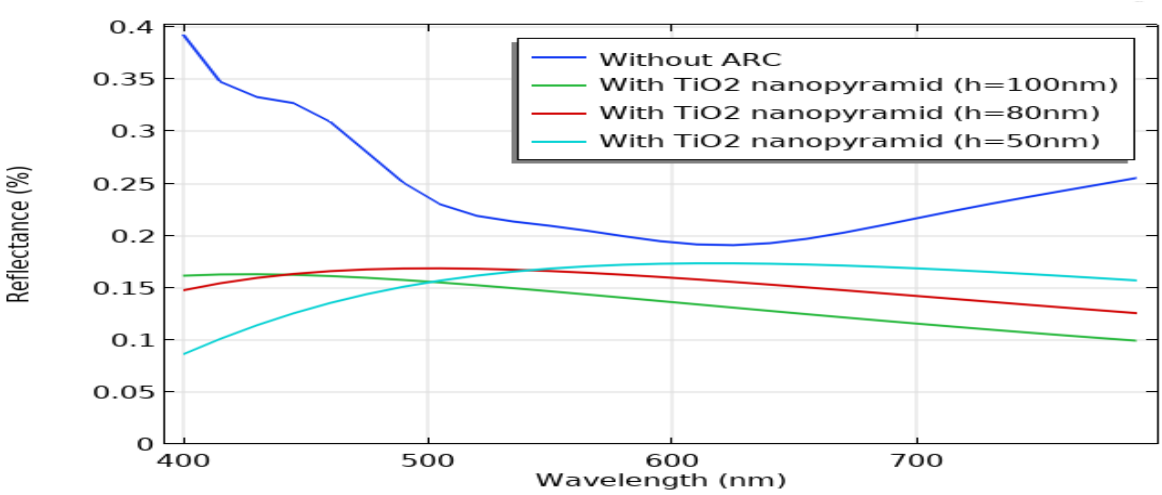

Figure 7: The reflectance percentage of $GaAs$ solar cell coated with TiO_2 nanopyramid at constant width

In the case of the cubic structure, the flat surfaces and shape edges create multiple internal reflections and varied surface topologies, which enhance its anti-reflection properties. It also scatters light in specific directions, which is advantageous for ARC design. However, designing a uniform cubic structure is challenging and may lead to non-uniform reflectivity and a narrower range of wavelengths. When optimizing the length of the cubic nanostructure to 50 nm, 80 nm, and 100 nm, the cube achieved the lowest percentage reflectance of 3.55%, 3.56%, and 3.60%, within the broad wavelength of 550nm and 650nm respectively. The 50 nm nanocube structure proved to be the most effective among the three structures, with a minimum percentage reflectance of 3.55%, as shown in Figure 8.

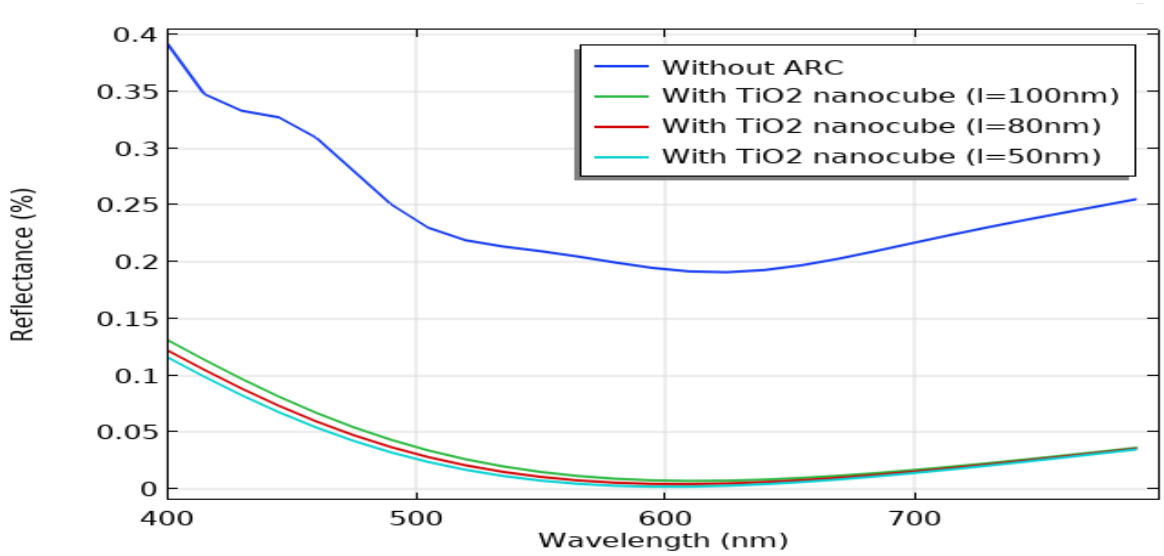

Figure 8: The reflectance percentage of $GaAs$ solar cell coated with TiO_2 nanocube

In comparison, among the three structures, the 50 nm cubic structure outperformed the others, followed by the pyramidal structure with dimensions of height = 100 nm and width = 50 nm, which also demonstrated a broad wavelength range, as shown in Figure 9.

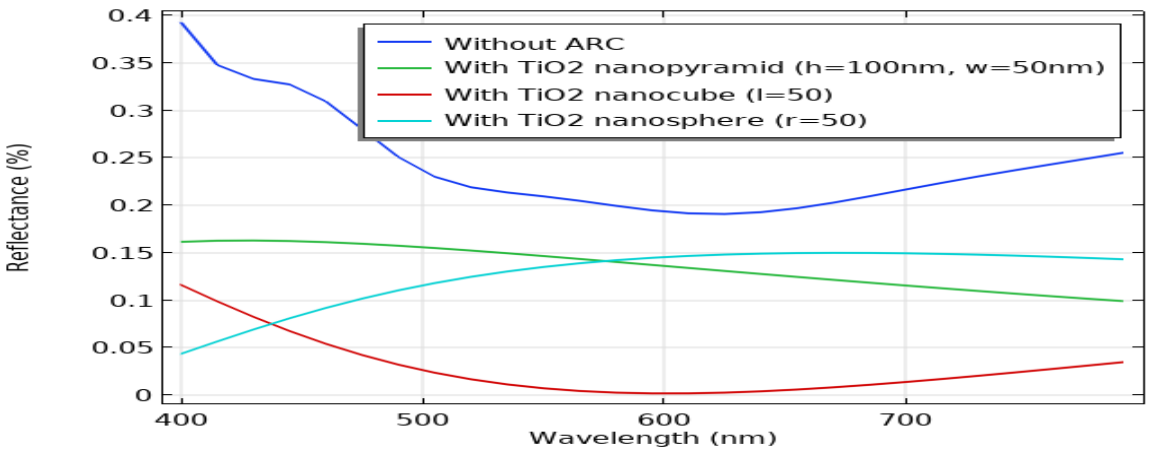

Figure 9: Best percentage reflectance of $GaAs$ solar cell coated with TiO_2 nanostructures

However, in comparison with other works as shown in Table 3. Abu-shamlah *et al.* (2021) simulated cubic TiO_2 nanostructure ARC using COMSOL software and obtained the percentage reflectance of 20.1% at 50nm and 0^0. Likewise, Woo *et al.* (2014) used TiO_2 sub-wavelength structures at the thickness of 50nm of cubic nanostructure and obtained 6.2%. In the case of Parajuli *et al,* (2023), the percentage reflectance of 5.0% at the thickness of 62nm length was obtained by using PC1D simulation software. This revealed that, 3.5% found by this work is the lowest and best value of percentage reflection that can enhance the absorption capacity of the solar cell and later improve the overall efficiency.

Table 3: Percentage reflectance of the three TiO_2 nanostructures coated on $GaAs$ solar cell

Shape	Parameter dimension	Percentage reflectance (%) (this work)	Percentage reflectance (%) (Abu-shamlah *et al, 2021*)	Percentage reflectance (%) (Woo *et al, 2014*)	Percentage reflectance (%) (Parajuli *et al, 2023*)
Cubic	l= 100nm l=80nm l=50nm	3.60 3.56 3.55	28.0 26.6 20.1	- - 6.2	- - 5.0 at 62nm
Pyramid At constant height of 80nm	w=100nm w=80nm w=50nm	14.3 14.9 15.7	- 14.4 14.4	- - -	- - -
Pyramid At constant width of 50nm	h=100nm h=80nm h=50nm	9.9 12.5 15.7	21.1 14.4 9.8	- - -	- - -
Sphere	r=35nm r=25nm r=50nm	15.2 15.7 14.3	11.9 9.2 23.5	- - -	- - -

ISSN: 3027-2335

5. Conclusion

We found that the cubic nanostructure, with the length of 50 nm at an angle of 70^0, demonstrated the most significant reduction in reflectance from 25.5% without ARC to 3.55%, followed by the pyramid nanostructure, with the ability to reduce reflectance to 9.9% at dimensions of 50 nm and 100 nm in width and height respectively. However, the spherical nanostructure revealed the less performance with the reflection reduction of 15.7% at the dimension of 25nm radius. The results indicated that increasing the height of the pointed tips of the pyramid shape minimized reflectance more effectively than increasing the edge width, and also, as the radius of the spherical nanostructure increased, the reflectance percentage also increased. These results can revealed potential of $Ti0_2$ material as an efficient ARC in broad ranges of wavelengths and incident angles for high performance photovoltaic devices for practical industrial applications.

Funding

This research did not receive any specific grant from funding agencies in the public, private, commercial, NGOs etc.

References

Abu-Shamleh, A., Alzubi, H., & Alajlouni, A. (2021). Optimization of antireflective coatings with nanostructured TiO2 for GaAs solar cells. *Photonics and Nanostructures - Fundamentals and Applications*, *43*. https://doi.org/10.1016/j.photonics.2020.100862

Domtau, D. L., Simiyu, J., Ayieta, E. O., Muthoka, B., & Mwabora, J. M. (2016). Optical and Electrical Properties Dependence on Thickness of Screen-Printed TiO 2 Thin Films. *Journal of Materials Physics and Chemistry*, *4*(1), 1–3. https://doi.org/10.12691/jmpc-4-1-1

Law, A. M., Jones, L. O., & Walls, J. M. (2023). The performance and durability of Anti-reflection coatings for solar module cover glass – a review. In *Solar Energy* (Vol. 261, pp. 85–95). Elsevier Ltd. https://doi.org/10.1016/j.solener.2023.06.009

Leem, J. W., Su Yu, J., Jun, D. H., Heo, J., & Park, W. K. (2014). Efficiency improvement of III-V GaAs solar cells using biomimetic TiO 2 subwavelength structures with wide-angle and broadband antireflection properties. *Solar Energy Materials and Solar Cells*, *127*, 43–49. https://doi.org/10.1016/j.solmat.2014.03.041

Makableh, Y. F., Alzubi, H., & Tashtoush, G. (2021). Design and optimization of the antireflective coating properties of silicon solar cells by using response surface methodology. *Coatings*, *11*(6). https://doi.org/10.3390/coatings11060721

Mandong, A. M., & Uzum, A. (2021). Fresnel calculations of double/multi-layer antireflection

coatings on silicon substrates. *Research on Engineering Structures and Materials*, *7*(4), 539–550. https://doi.org/10.17515/resm2020.241en1217

Mbengue, N., Diagne, M., Dia, F., Ndiaye, S., Niasse, O. A., Dieye, A., Niane, M., & Ba, B. (2016). *Simulation Study of Optical Reflection and Transmission Properties of the Anti-Reflection Coatings on the Silicon Solar Cells*. https://doi.org/10.17950/ijset/v5s3/308

Parajuli, D., Gaudel, G. S., Kc, D., Khattri, K. B., & Rho, W. Y. (2023). Simulation study of TiO2 single layer anti-reflection coating for GaAs solar cell. *AIP Advances*, *13*(8). https://doi.org/10.1063/5.0153197

Rathanasamy, G.V. Kaliyannaa, S. Sivaraj, A. Saminathan, B. Krishnan, D. Palanichamy, R. E. U. (2022). Influence of Silicon Dioxide-Titanium Dioxide Antireflective Electrosprayed Coatings on Multicrystalline Silicon Cells. *Advances in Materials Science and Engineering*, *2022*. https://doi.org/10.1155/2022/9444524

Richards, B. S. (2003). Single-material TiO2 double-layer antireflection coatings. *Solar Energy Materials and Solar Cells*, *79*(3), 369–390. https://doi.org/10.1016/S0927-0248(02)00473-7

Shanmugam, N., Pugazhendhi, R., Elavarasan, R. M., Kasiviswanathan, P., & Das, N. (2020). Anti-reflective coating materials: A holistic review from PV perspective. *Energies*, *13*(10), 1–93. https://doi.org/10.3390/en13102631

Wang, X., & Shen, J. (2010). Sol-gel derived durable antireflective coating for solar glass. *Journal of Sol-Gel Science and Technology*, *53*(2), 322–327. https://doi.org/10.1007/s10971-009-2095-y

Womack, G., Kaminski, P. M., Abbas, A., Isbilir, K., Gottschalg, R., & Walls, J. M. (2017). Performance and durability of broadband antireflection coatings for thin film CdTe solar cells. *Journal of Vacuum Science & Technology A: Vacuum, Surfaces, and Films*, *35*(2). https://doi.org/10.1116/1.4973909